J Mater Sci (2006) 41:4440–4444
DOI 10.1007/s10853-006-0090-z

Nanosecond time resolved electron diffraction studies of the $\alpha \rightarrow \beta$ in pure Ti thin films using the dynamic transmission electron microscope (DTEM)

Thomas LaGrange · Geoffrey H. Campbell · Jeffrey D. Colvin · Bryan Reed · Wayne E. King

Received: 16 December 2005 / Accepted: 2 March 2006 / Published online: 28 June 2006

Abstract The transient events of the α–β martensitic transformation in nanocrystalline Ti films were explored via single-shot electron diffraction patterns with 1.5 ns temporal resolution. The diffraction patterns were acquired with a newly constructed dynamic transmission electron microscope (DTEM), which combines nanosecond pulsed laser systems and pump-probe techniques with a conventional TEM. With the DTEM, the transient events of fundamental material processes can be captured in the form of electron diffraction patterns or images with nanosecond temporal resolution. The transient phenomena of the martensitic transformations in nanocrystalline Ti is ideally suited for study in the DTEM, with their rapid nucleation, characteristic interface velocities ~1 km/s, and significant irreversible microstructural changes. Free-standing 40-nm-thick Ti films were laser-heated at a rate of ~10^{10} K/s to a temperature above the 1155 K transition point, then probed at various time intervals with a 1.5-ns-long, intense electron pulse. Diffraction patterns show an almost complete transition to the β phase within 500 ns. Post-mortem analysis (after the sample is allowed to cool) shows a reversion to the α phase coupled with substantial grain growth, lath formation, and texture modification. The cooled material also shows a complete lack of apparent dislocations, suggesting the possible importance of a ''massive'' short-range diffusion transformation mechanism.

T. LaGrange (✉) · G. H. Campbell · J. D. Colvin · B. Reed · W. E. King
Chemistry and Materials Science, Lawrence Livermore National Laboratory, Livermore, CA 94550, USA
e-mail: lagrange2@llnl.gov

Introduction

Martensitic transformations have been studied for over a century, and current understanding of these rapid transformations is still limited to phenomenological models based on post-mortem observations of crystallographic relationships between the parent and product phases [1]. These limitations stem from the inability to observe the transformation directly due to the inherent rapid growth rates and interface velocities that can be on the order of 10^3 m/s. In spite of this, some kinetic models have been developed for alloy systems that exhibit time-dependent growth (isothermal) and have slow nucleation and growth rates [1, 2]. The development of more sophisticated models that extend to other kinetic modes of the martensitic transformation, such as athermal modes, necessitates a technique that has both high spatial and high temporal resolution. One such instrument has been constructed at Lawrence Livermore National Laboratory (LLNL), the dynamic transmission electron microscope or DTEM. This provides a means to observe the dynamics of rapid material processes such as the martensitic transformation.

The LLNL DTEM is a next-generation version of instruments developed at Technische Universität Berlin [3], but with better time resolution, and improved electron optics. The high temporal resolution in DTEM is accomplished by using short, intense packets of electrons to illuminate the specimen. The electron pulses are generated via photoemission by irradiating a photocathode with nanosecond UV laser pulses. Each packet contains ~10^7 electrons, sufficient to produce a good-quality diffraction pattern with a single shot from a small region (~5 μm in diameter). The related technique of ultrafast electron diffraction (UED) has typically had to average a large number of shots (with ~10^5 electrons each) over an area ~100 μm

in diameter [4]. The DTEM thus has an advantage both in spatial resolution and in the study of processes that cannot be driven reversibly.

Typical DTEM time-resolved experiments involve pumping a TEM specimen with a short laser pulse to induce transient heating or high-pressure states and probing these transient states with a synchronized photo-electron pulse (Fig. 1). Since this technique is coupled to a standard TEM column, data can be collected in the form of images or diffraction patterns. Furthermore, different delays can be set between the pump and probe pulses, and the entire evolution of the material process can be delineated, which makes the DTEM attractive for studying rapid phase transformations such as the $\alpha \rightarrow \beta$ transition in Ti.

Upon heating above the characteristic martensitic start temperature of 1155 K, Ti transforms from the HCP, α-phase to the BCC coordinated, β-phase that is stable up to the melting temperature (1936 K). The broad temperature ranges for which the α and β phases are stable make Ti an appropriate choice for the DTEM based experiments. Moreover, the transformation is speculated to be rapid in nanocrystalline thin films, like those used in this study, due to the high number of heterogeneous nucleation sites per volume. Using single-shot diffraction with nanosecond time resolution, preliminary investigations of the transformation were conducted. These results will be discussed in conjunction with post-mortem microstructure investigations of the laser treated Ti films.

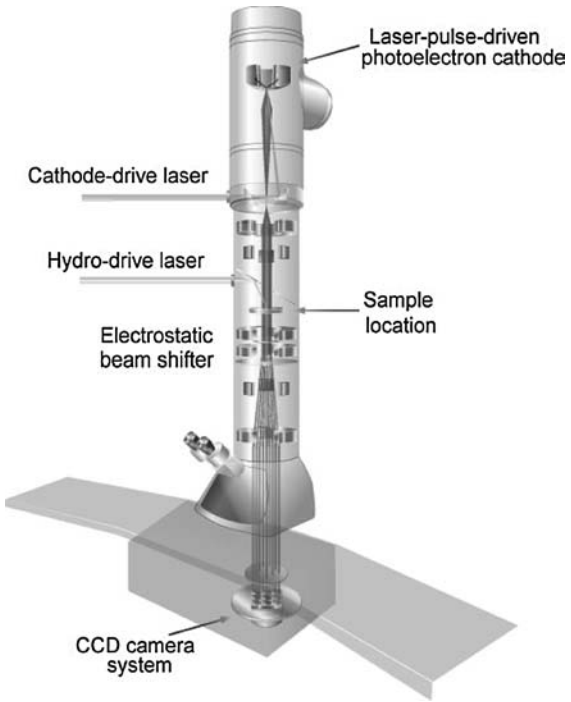

Fig. 1 Schematic of LLNL DTEM

Materials and methods

Pure Ti thin films with a thickness of 40 nm were fabricated by sputter-deposition onto NaCl single-crystalline substrates heated to 573 K. As-deposited films were sectioned into 2 mm × 2 mm squares by cleaving the crystal along (100) planes of the NaCl crystal. These sections were placed into distilled water to release the film from the salt substrate, and the resulting free-standing films were then floated onto 150-mesh copper TEM grids. The Ti films were nanocrystalline with grain sizes ranging from 50 to 100 nm and were highly textured (see Fig. 2a). Electron diffraction simulation of the HCP structure (Fig. 2b) indicated that the grains were preferentially oriented to the $[10\bar{1}1]$ zone axis and had two in-plane orientation variants rotated 90° with respect to each other about the foil normal.

In situ observations of the phase transformation were performed in the DTEM. Table 1 lists the respective parameters of laser systems and photo-electron pulses. The present capabilities of the DTEM limit data acquisition to the diffraction mode, since the number of electrons per pulse (10^7) is too low to produce interpretable (low noise) single shot images[1]. Therefore, transformation kinetics were only studied by a series of electron diffraction patterns acquired at different delays between the pump laser and electron probe pulses. At present, only one single-shot diffraction pattern can be acquired for each pump laser heating pulse. Since it was observed that the microstructure was modified significantly after one laser shot and the transformation kinetics are on dependent the initial microstructure, for consistency, a new region was studied for each pump-probe experiment and the results compared. This was applicable since the films used in this study had a uniform thickness and a homogenous microstructure. All of the diffraction patterns were taken at the same camera length, beam convergence and current and acquired as 16-bit Tiff images using a 2k by 2k CCD binned by 4. The raw diffraction pattern data were rotationally, and radial intensity was plotted with reciprocal lattice spacing.

Results

Before presenting time-resolved patterns, it is useful to first show the effects of laser irradiation on the nanocrystalline Ti microstructure. Post-mortem TEM observation of laser-treated films revealed that the film underwent substantial grain growth and morphological changes. The comparison of Fig. 3a and b clearly shows the dramatic increase in grain size.

[1] Single-shot imaging requires 10^6–10^8 detected electrons per pulse, depending on the contrast formation mechanism and desired observation. In the present study, it is estimated that 5×10^7 e/pulse are needed for appropriate imaging.

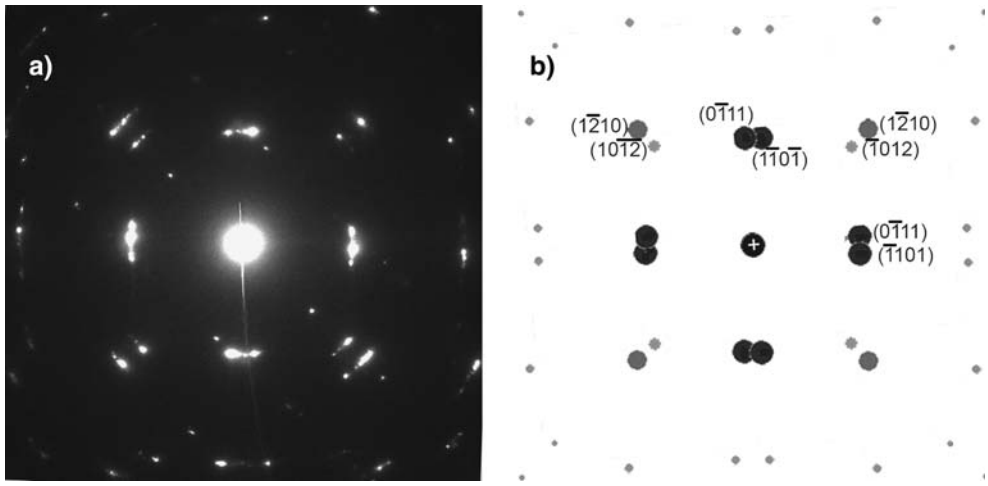

Fig. 2 (**a**) Static experimental electron diffraction pattern, (**b**) two simulated [10$\bar{1}$1] Z.A. electron diffraction patterns rotated 90° with respects to each other. The simulation was computed using JEMS©

Table 1 Laser and electron pulse parameters

	Pulse energy range	Wavelength (nm)	Pulse duration FWHM (ns)	Spot size FWHM (μm)
Photo cathode laser	10 nJ–1 mJ	213	3	10^3
Specimen treatment laser	10 nJ–300 mJ	1064	70	70 × 110*
Electron pulse	10^7 e^- per pulse	0.00251	1.5	4**

* Since the incident beam is 35° to the specimen normal, the projected beam is elliptical

** The table indicates the smallest possible electron illumination diameter, using the lowest C1 lens excitation setting (which optimized the total charge per pulse). The C1 setting was not varied in the experiments

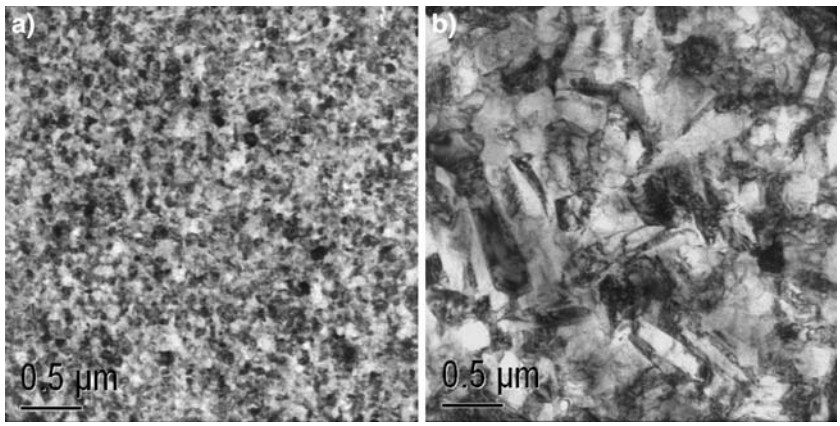

Fig. 3 (**a**) As-deposited Ti-film microstructure, (**b**) after laser treatment

Interestingly, the laser treated films exhibit two main grain morphologies, small ''pancake'' grains and large laths, where the pancake grains straddle the ''packets'' of laths. Another notable feature is the lack of dislocations in the post-treated lath microstructure, which are commonly observed in bulk materials [1, 2, 5, 6], but may not exist in film cycled with extreme heating and cooling rates. To estimate the heating rates in 40-nm thick films, heating curves were calculated using a 1-D lagrangian hydrodynamics simulation[2] and pump laser parameters listed in Table 1 for two different laser energies, 21 and 56 μJ. The predicted heating rates (10^{10} K/s and 2.4×10^{10} K/s, respectively) are remarkably high compared to traditional bulk studies (by seven orders of magnitude [7]) but are easily accessed in the case of thin-film short-pulse-laser experiments.

Figure 4a shows a typical single-shot diffraction pattern for a textured, nanocrystalline Ti film. The pattern is similar to conventional TEM SADP shown in Fig. 2a, although the spots are slightly broader, since the electron beam was converged in order to increase the signal. It should also be noted that numerous high-order reflections are present and the quality of the pattern is higher than those recently

[2] The 1-D approach was used to reduce computing time and was assumed valid based on the argument that electron probe size is much smaller than incident laser spot size.

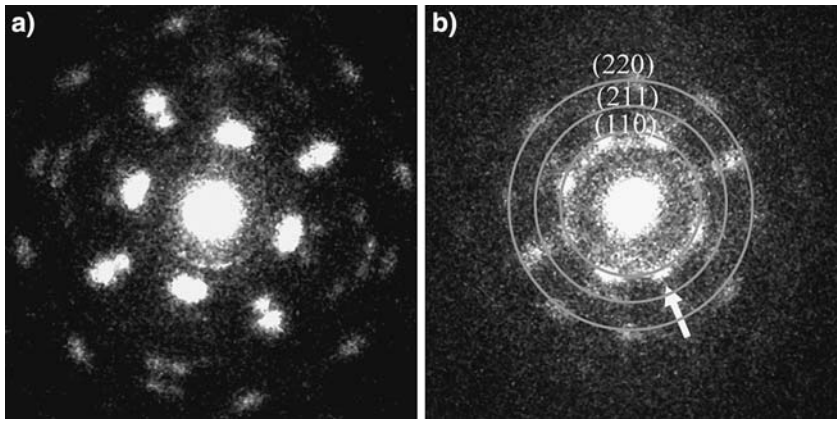

Fig. 4 Single shot diffraction patterns recorded with 1.5 ns time resolution, (**a**) HCP structure acquired at room temperature before laser treatment, (**b**) indexed as BCC structure and was acquired 500 ns after the 15 μJ pump laser pulse. Arrow indicates the appearance of new spots that did not exist in the HCP pattern

acquired for similar Ti films using the TU Berlin instrument, where only the first-order reflections are clearly visible [8]. Second and third reflections are present, which facilitate the deconvolution of the BCC and HCP phases and the study of transformation evolution from α to β. Figure 4b shows the time-resolved diffraction pattern of the crystal structure 500 ns after a 15 μJ laser pulse hit the foil. The concentric rings overlaid on the diffraction pattern show that the crystal structure was primarily BCC. The change in crystal structure is especially notable by the appearance of the new diffraction spots, as indicated by the white arrow in Fig. 4b. A clearer depiction of the change in phase was performed by taking the difference pattern (Fig. 5a) of the two diffraction patterns in Fig. 4, and plotting the radial averaged intensity of difference pattern with reciprocal lattice units (*d*-spacing). The peaks present in Fig. 5b show that it is indeed BCC. There was approximately 75 ± 5% BCC, β-phase present in Fig. 4b, which was calculated first by fitting the peaks in Fig. 5b with a Lorentzian profile function and determining their integrated intensities that were then compared with the integrated intensities of difference pattern containing only HCP reflections (Figs. 4b–5a).

Figure 6a shows the single-shot diffraction of same region after the material has cooled to room temperature (which takes less than a millisecond). The diffraction spots in this image are sharper, which indicates grain coarsening as observed in Fig. 3. The pattern also exhibits spots that are not present before laser heating, and some that appear to emanate from the prior β-phase texture. After this pattern was acquired, the region was hit with a second 30 μJ laser pulse that was sufficient to induce melting at 100 ns after impact (apparent from the diffuse ring in Fig. 6b). This study offers both a temperature calibration and means to validate the laser-absorption simulations. Unfortunately, the simulations overestimate the requisite energy by more than 40%, and work is in progress to bring the simulation and experiment into coincidence and to better estimate the heating rates.

Discussion

It first should be noted that the phenomenal grain growth observed in the post-mortem TEM studies occurs at time scales less than a millisecond. The extensive grain growth

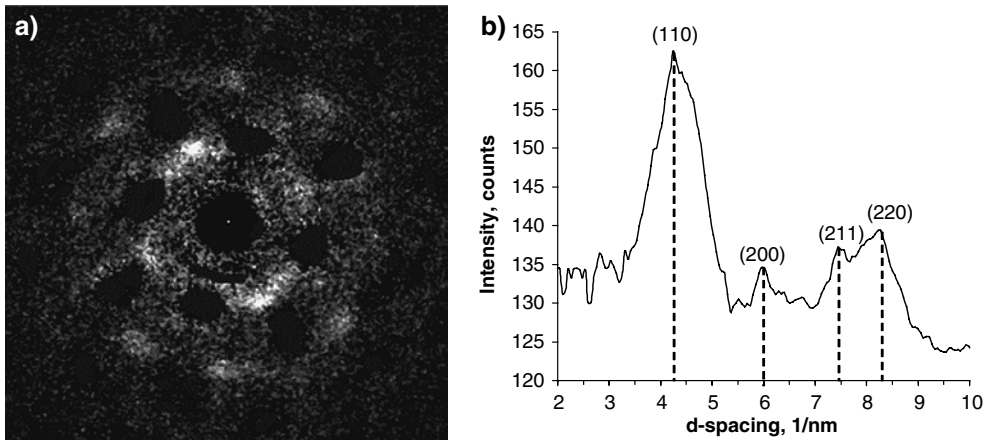

Fig. 5 (**a**) Difference pattern showing between Figs. 6a and b, showing residual BCC reflections, (**b**) radial intensity versus *d*-spacing for the rotational averaged pattern in Fig. 5a

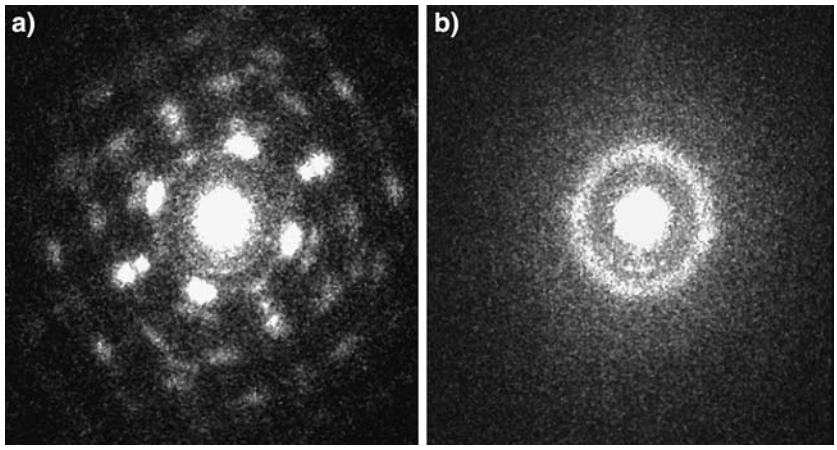

Fig. 6 Single shot diffraction patterns recorded with 1.5 ns time resolution, (**a**) acquired at room temperature after laser treatment, HCP structure as indexed in Fig. 2. The diffraction pattern in (**b**) was acquired 100 ns after a 30 μJ pump laser pulse, which was sufficient to induce melting

most likely occurs in the β phase, where films are expected to be at high temperature (~1200 K) for extended times (>5 μs) [9]. However, the appearance of the smaller pancake grains may indicate recrystallization and growth in the α phase as well.

The additional spots observed in Fig. 6 are linked with the formation of laths and randomization of the microstructure. Randomization of the microstructure is expected since 12 hexagonal variants can form for each BCC crystal variant and the texture of the prior structure is partially lost due to the nucleation and growth of different HCP variants. The high dislocation densities typically occur by cycling through the α to β transformation [5]. However, dislocations were not apparent in the lath microstructure of the laser treated films, which is intriguing. The nucleation of dislocations in the parent matrix typically accompanies martensitic transformations and acts to relieve the stress caused by the nucleating martensite variant (strain energy minimization) [2, 5, 6]. However, the extremely high heating and cooling rates in the experiment may inhibit the slower dislocation nucleation processes. It is also possible that dislocation formation may not be necessary due to large free surfaces that relieve the excess strain energy.

The second possibility is that laths form from an incoherent nucleation and growth mechanism requiring diffusion, such as a massive transformation, which would also explain the randomization of the microstructure. In the absence of impurities, like Fe that strongly inhibit diffusion, pure Ti can undergo a massive type transformation at fast cooling rates [7]. A further argument is that high concentrations (>1 at.%) of oxygen, which is an α stabilizer, can favor a massive type transformation mode, which may exist in nanocrystalline films. However, this requires more investigation. Observing the interfaces through single-shot imaging during the transformation would certainly help to divulge the mechanism.

Conclusions

The HCP αTi films were transformed rapidly to BCC phase using 80 ns, 1064 nm, 15 μJ laser pulses. Ex situ examinations showed extreme grain growth after only one laser hit and in time scales on the order of microseconds. The reason for the lack of dislocations in the lath microstructure is not clear, and more experiments using single-shot time resolved imaging are needed to further illuminate the transformation mechanisms in Ti thin films. Clearly, the preliminary results show the capabilities of the LLNL DTEM for time resolved diffraction based experiments. Future studies in the DTEM will unveil fundamental materials science processes on time and length scales not previously accessible by other techniques.

Acknowledgements This work performed under the auspices of the U.S. Department of Energy by the University of California, Lawrence Livermore National Laboratory under Contract No. W-7405-Eng-48. I would like to thank Ben Pyke and Rich Shuttlesworth for their hard work and dedication in the design and construction of the DTEM.

References

1. Smith CS (1992) Martensite. ASM International, p 21
2. Raghavan V (1992) Martensite. ASM International, p 197
3. Bostanjoglo O, Elschner R, Mao Z, Nink T, Weingärtner M (2000) Ultramicroscopy 81(3–4):141
4. King WE, Campbell GH, Frank A, Reed B, Schmerge JF, Siwick BJ, Stuart BC, Weber PM (2005) J Appl Phys 97:111101
5. Lütjering G, Williams JC (2003) Titanium. Springer-Verlag, Berlin, Heidelberg, New York, p 27
6. Oh MS, Lee JY, Park JK (2004) Metall Mater Trans A 35A:3071
7. Cormier M, Claisse F (1974) J Less-Common Metals 34:181
8. Kleinschmidt H, Ziegler A, Campbell GH, Colvin JD, Bostanjoglo O (2005) J Appl Phys 98:054313
9. Campbell GH, Lagrange TB, King WE, Colvin JD, Ziegler A, Browning ND, Kleinschmidt H, Bostanjaglo O (2005) In: Howe JM, Laughlin DE, Lee JK, Dahmen U, Soffa WA (eds) Proc. Solid-Solid Phase Trans. Inorg. Mater. Conf. 2005, vol 2. TMS, Warrendale PA, p 443